AAPS PharmSciTech, Vol. 16, No. 5, October 2015 (© 2015)
DOI: 10.1208/s12249-015-0310-4

Research Article

The Design of Nanostructured Metronidazole-Loaded HPC/Oxide Xerogel Composites: Influence of the Formulation Parameters on *In Vitro* Characterisation

Katarzyna Czarnobaj[1,2]

Received 2 December 2014; accepted 6 February 2015; published online 26 February 2015

Abstract. In this study, oxide and polymer/oxide xerogels with metronidazole were prepared and examined as carriers of drug for the local application to the bone. The nanoporous SiO_2–CaO–P_2O_5 and HPC–SiO_2–CaO–P_2O_5 xerogel materials with different amounts of the polymer [hydroxypropyl cellulose (HPC)] were prepared using the sol–gel technology, and their physicochemical properties were characterised with respect to chemical structure [by Fourier transform infrared spectroscopy (FTIR)], porosity and the specific surface area of solids (BET), crystallinity [by X-ray powder diffraction (XRD)], morphology [by scanning electron microscope (SEM)] and the *in vitro* release of the metronidazole over time (by UV–vis spectroscopy, in the ultraviolet light region). HPC-modified oxide xerogels as the carriers of drug showed slower release of metronidazole, due to the structure and stronger interactions with drug as compared with the pure oxide xerogel. Kinetic analysis indicated diffusional mechanism of drug release from all xerogel carriers. HPC addition to the oxide material resulted in a decrease in the porosity and improved the bioactive properties of xerogels. Obtained results for xerogel composites suggest that the metronidazole-loaded xerogels could be attractive candidates for local delivery systems particularly to a bone.

KEY WORDS: drug delivery systems; nanostructured composites; porous materials.

INTRODUCTION

The use of bioactive materials and the design of alternative drug delivery dosage forms are the important aims to improve the efficiency of the treatment and to decrease its side effects. The delivery of the drug to its specific target organ (e.g. to the bone) provides optimal concentration and accumulation of drug in the infection site without its dispersing across the entire body.

The sol–gel prepared nanostructured xerogels are excellent candidates for a sustained release drug delivery device (1–4). Using the sol–gel method, it is possible to obtain materials with a similar chemical composition to the bone (such as hydroxyapatite). The main area of applications of these materials is orthopaedic, both in the bone defects regeneration and in the treatment of bone disease. This is due to their high bioactivity (the ability to form chemical bonds with bone tissue) and porosity (ability to incorporate of drug substances inside these materials, and release of drugs in controlled, prolonged manner) (5–7).

The sol–gel process requires metal alkoxide or salt, alcoholic solution and water. The hydrolysis and condensation of the liquid substrates create the three-dimensional, continuous solid oxide network (sol–gel transformation) (8–10). The sol–gel method is used for the production of amorphous glassy materials—xerogels. Drug substances in solid form or as a solution are homogeneously dispersed in the liquid sol, and physically entrapped in the formed solid oxide network. Sol–gel processing is classified as a technique that can produce amorphous pure oxides (e.g. SiO_2), mixed oxides by partially replacing silica with CaO, P_2O_5, TiO_2 and ZrO_2, or inorganic–organic hybrid materials by co-condensation silica with organic components [e.g. polydimethylsiloxane (PDMS), hydroxypropyl cellulose (HPC)] (11,12).

Moreover, sol–gel procedure is well known for a valuable set of properties, such as the low temperature of the chemical process, high homogeneity and purity of obtained products, their non-toxicity and biocompatibility *in vivo* (1,5). They are also bioactive, in particular if they contain calcium and phosphorus in its composition (e.g. SiO_2–CaO–P_2O_5). One of the main drawbacks of oxide xerogels is their brittleness. Therefore, one of the most important goals when preparing the xerogels is to achieve better mechanical performance of the finished material. This aim can be achieved by introducing the flexible polymer chains into the oxide network. The organic components are introduced into the liquid alkoxide where they are co-condensed with the molecules of hydrolysed alkoxides. Organic modification in the oxide network changes its structural parameters, especially porosity and chemical prop-

[1] Department of Physical Chemistry, Medical University of Gdańsk, al. Gen. J. Hallera 107, 80-416, Gdańsk, Poland.
[2] To whom correspondence should be addressed. (e-mail: kczar@gumed.edu.pl)

erties of material (e.g. hydrophilicity, adhesion) (13,14). Additionally, the organic/inorganic composites are often much more closely related to biological structures.

In the present work, SiO_2–CaO–P_2O_5 and HPC-modified SiO_2–CaO–P_2O_5 with different amounts of polymer within the oxide network have been successfully synthesised via sol–gel route using tetramethoxysilane [Si $(OCH_3)_4$], triethyl phosphate [PO $(OEt)_3$], calcium chloride and HPC as organic modifier of oxide network. This polymer was selected due to its excellent biocompatibility, bioadhesion, appropriate mechanical properties and osteoconductivity providing more support for hard tissue (15).

The structural, textural and bioactive properties of the obtained materials were investigated by Fourier transform infrared spectroscopy (FTIR), Brunauer–Emmett–Teller (BET), scanning electron microscope (SEM) and X-ray diffraction (XRD) techniques. In addition, this study examined the possibility of using HPC/oxide xerogels as a controlled release drug carriers. Due to the weak blood supply of bone tissue and the poor penetration of drug to the bone, the implantable drug delivery seems to be a very attractive solution. This form of drug offers a shorter period of the pharmacological treatment of bone disease, providing locally optimal the drug concentration and avoiding systemic toxic effects.

Metronidazole, a chemotherapeutic substance of the group of derivatives of 5-nitroimidazole, was chosen as the model drug for preparing the drug delivery systems. Metronidazole exhibits protozoicidal and anaerobicidal effect. For this reason, metronidazole is often used to treat infections of the bones, joints, and periodontium. It is also used in perioperative prophylaxis upon grafting bone and teeth implants (16).

The drug was added to the liquid precursors of carriers. During carrier gelation, drug was entrapped within the formed solid. Subsequently, *in vitro* release behaviour of metronidazole from sol–gel processed composites was determined in simulated body fluid (SBF).

MATERIALS AND METHODS

Tetramethoxysilane (TMOS, $C_4H_{12}O_4Si$), calcium chloride ($CaCl_2$), triethyl phosphate (TEP, PO $(OC_2H_5)_3$), hydroxypropyl cellulose (HPC, average M_w: ~80,000) and drug—metronidazole, 2-methyl-5-nitroimidazole-1-ethanol (MT) (Sigma-Aldrich Co., Poznań, Poland) were used without further purification. Methanol and hydrochloric acid (POCh Co., Gliwice, Poland) were of analytical grade purity.

SBF as the dissolution medium for release analysis and bioactivity test was prepared according to Kokubo *et al.* (17,18).

Xerogels Preparations

Three different types of xerogels (Table I) were prepared through the sol–gel processing.

In order to obtain SiO_2–CaO–P_2O_5 xerogel material mixed with a model drug—metronidazole—at the beginning of synthesis, silica sol was obtained. For this purpose, the methanol solution of tetramethoxysilane (as a silica precursor) with water (molar ratio TMOS/H_2O=1:4) was vigorously stirred at room temperature for 3 h to the complete reaction of hydrolysis and condensation of alkoxide. HCl (0.1 M) was used as a catalyst for the hydrolysis reaction. Separately, calcium–phosphorus sol was prepared from calcium chloride and triethyl phosphate. The methanol solution of TEP was hydrolysed with distilled water under vigorous stirring for 24 h. Then, a methanol solution of $CaCl_2$ was added drop-wise into the hydrolysed phosphate sol. Both calcium and phosphate solutions were mixed together for 1 h in the molar proportion Ca/P=1.67 typical of hydroxyapatite (19).

The resulting solution was finally added to the silica sol to give a concentration of 20 vol.%. MT was added into the silica solution after 1 h condensation and then continuously stirred to the gelation.

HPC/SiO_2–CaO–P_2O_5 xerogels were obtained in an analogous manner to SiO_2–CaO–P_2O_5 one. First, the silica–calcium–phosphorus sol was obtained as described above. Next, HPC was added to the obtained sol solution. The concentration of HPC in oxide xerogels was 10 and 20 vol.%.

Subsequently, all wet gels were heated at 50°C for 3 h to obtain the solid xerogels. The final materials were in the form of a translucent, crack-free monoliths containing drug in an amount of 10 mg/g xerogel.

Characterisations

FTIR spectra of xerogels were obtained using an FT/IR-410 spectrometer, Jasco, in pressed KBr discs. The spectra were collected over a range of 4000–400 cm^{-1} (64 scans; resolution, 4 cm^{-1}).

The chemical stability of the xerogels were monitored using the pH-meter Lab 860 (SI Analytics GmbH) and the conductometer Lab 960 (SI analytics GmbH), by measuring the pH and conductivity of the SBF solution in which the xerogel samples were incubated, in a water bath at 37±0.1°C for the period of 3 months.

Surface area, pore volume and pore diameter of the xerogels were determined using a Micromeritics ASAP 2405N instrument and the Barret–Joyner–Halenda (BJH) methods.

The mechanical compressive strength of the xerogels was determined using an Erweka TBH 125 hardness tester.

XRD spectra were taken with an Empyrean/PANalytical XRPD diffractometer using Cu$K\alpha_1$ radiation at 20 kV and 40 mA.

SEM energy dispersive spectroscopy (SEM-EDS) analysis was carried out using a Quanta 3D FEG/FEI SEM, equipped with an EDS and a mapping detector.

UV–vis spectra were recorded on a Shimadzu UV-1800 spectrometer at room temperature.

Release Studies

Prior to the release experiments, the samples of xerogels were crushed and sieved to a desired diameter of granules, 1.6–2 mm. The xerogel samples (0.5 g) were soaked in 50 mL of SBF as the dissolution medium and were shaken in the thermostated shaking water bath (Julaba, Germany, 50 spm) at 37°C (±0.5°C). The concentration of MT in SBF was measured by the proposed spectrophotometric method (λ=320 nm) by taking 2 mL of the solution at selected intervals based on the drug

Table I. Composition Design of the Xerogel Composites

Xerogel		Composition							
		TMOS (g)	TEP (g)	$CaCl_2$ (g)	HPC (g)	MeOH (mL)	2%HCl (mL)	H_2O (mL)	MT (mg)
A	SiO_2–CaO–P_2O_5	12.65	1.15	1.4	–	50	0.5	10.5	61.5
B	SiO_2–CaO–P_2O_5–10%HPC	12.65	1.15	1.4	0.7	50	0.5	10.5	83.8
C	SiO_2–CaO–P_2O_5–20%HPC	12.65	1.15	1.4	1.55	50	0.5	10.5	96

release. The release medium was replaced by a fresh SBF solution (2 mL) in order to maintain a volume of 50 mL. The amount of MT obtained from the drug release studies was calculated from a linear regression equation.

RESULTS AND DISCUSSION

Carriers of MT

Innovative ways are needed to improve the delivery of drugs and to reduce their risk for side effects. Many local drug delivery systems have been investigated in the past. Bone implants as drug carriers show three significant advantages over the traditional treatment. First, they can be implanted into hard tissue such as bone resulting in drug isolation from the surrounding environment. This can minimise any interaction of the drug with healthy tissue and extend its half-life time by protecting the drug from premature activation and degradation. Second, they can deploy the drug directly into the target areas and thus lower the amount of drug needed. Third, they can release the drug at a slower rate. Consequently, these delivery systems have more manageable safety profile than the traditional treatment.

These results show that oxide and HPC/oxide xerogels also have great potential in local delivery of MT. Due to their biocompatibility and bioactivity, the oxide-based xerogels can interact with living bone and, therefore, be used in implantology and bone repair applications. Through interfacial reactions, these xerogels can develop a hydroxyapatite surface in contact with biological fluids (so-called bioactivity) that allows them to chemically bond to the host bone (20).

The SiO_2–CaO–P_2O_5 oxide system was selected due to the presence of calcium and phosphorus with similar chemical composition to that of bone (Ca/P=1.67). HPC, a biocompatible polymer, was added to make the xerogels more ductile, compared to the brittle oxides and bioadhesive. Additionally, in contact with an aqueous solution, hydration of HPC results in the formation of a viscous gel layer, what should minimise penetration of water inside the composite material and therefore should delay release of the drug substance.

Chemical Structure and Morphology of Composite Xerogels

The xerogels, pure oxides and modified with HPC were characterised using the FTIR technique as illustrated in Fig. 1. The FTIR analysis showed that the oxide xerogels were completely hydrolysed and well polymerised. The observed strong bands were caused by the vibrations of Si–O–Si groups at 1076, 924 and 800 cm^{-1} indicative of a high degree of polymerisation. The lack of bands derived from the CH

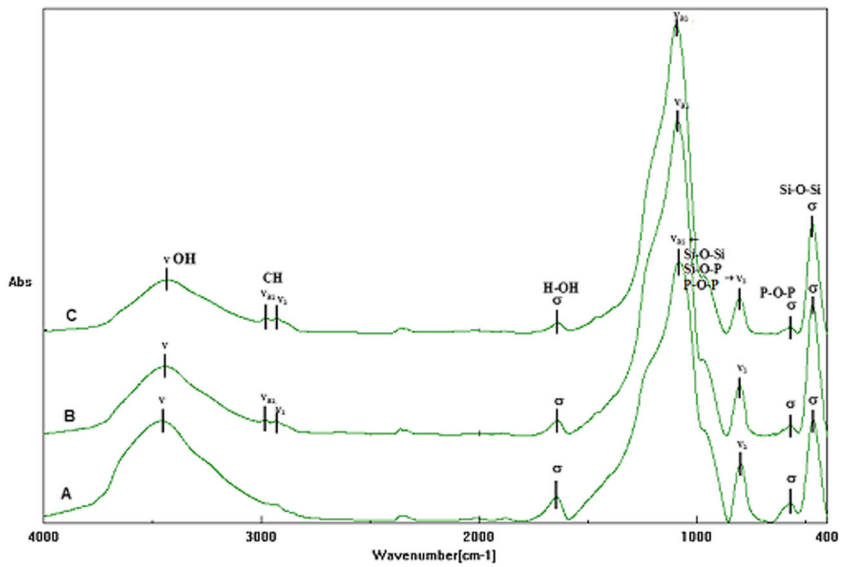

Fig. 1. FTIR spectra of SiO_2–Ca–P_2O_5 (**a**), HPC (10%)–SiO_2–CaO–P_2O_5 (**b**), and HPC (20%)–SiO_2–CaO–P_2O_5 (**c**) xerogels

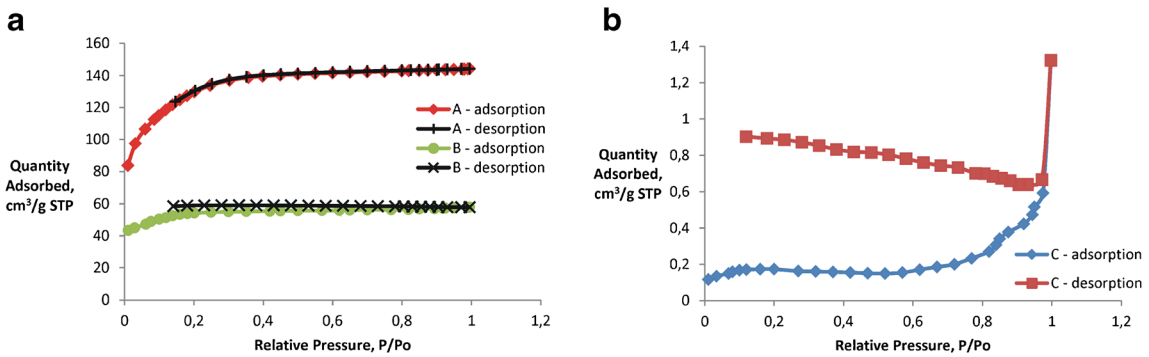

Fig. 2. Nitrogen adsorption–desorption isotherms of xerogels: **a** SiO_2–CaO–P_2O_5 (*A*), HPC (10%)–SiO_2–CaO–P_2O_5 (*B*) and **b** HPC (20%)–SiO_2–CaO–P_2O_5

stretching vibrations in the region of 2800 cm^{-1} indicates complete hydrolysis of the alkoxy- groups ($-OCH_3$, $-OC_2H_5$) derived from tetramethoxysilane and triethyl phosphate. Two broad bands—one at 3450 cm^{-1} and the other at 1631 cm^{-1}—were caused by O–H vibrations of Si–OH and P–OH groups and the water molecule retained in the pores of the oxide network.

The FTIR spectrum of the oxide xerogels modified with HPC was slightly different from the spectrum of the pure oxide xerogel. Additional bands were visible in the 2900–2800 cm^{-1} region. These bands originated from the C–H vibrations of the alkyl group derived from HPC (21).

The evaluations of the xerogels textural properties were conducted by the BET technique by nitrogen multilayer adsorption measured as a function of relative pressure.

As shown in Fig. 2a, SiO_2–CaO–P_2O_5 and SiO_2–CaO–P_2O_5–10%HPC xerogels showed isotherms of type I with a sharp initial increase in the adsorbed gas volume at a low relative pressure p/p_o, characteristic of microporous materials (pore diameter <2 nm) (22,23). The isotherm for the SiO_2–CaO–P_2O_5–20%HPC (Fig. 2b) indicates that this xerogel is characterised by very small values of adsorption, resulting from the very small surface area. These results prove that this material is macroporous—practically non-porous.

As presented in Table II, HPC addition to the oxide xerogel changes porosity parameters. SiO_2–CaO–P_2O_5 and SiO_2–CaO–P_2O_5–10%HPC xerogels differ significantly in terms of pore volumes and surface area values, whereas pore diameters are similar. For SiO_2–CaO–P_2O_5–20%HPC, the amount of introduced HPC resulted in nearly complete filling of pores. A large decrease in the specific surface area (from 444 to 0.51 $m^2\ g^{-1}$) and total pore volume (from 0.223 to 0.002 $cm^3\ g^{-1}$) with an increase in HPC content (up to 20 wt-%) indicates a reduction in the porosity of composites. This effect may be associated with the penetration of the polymer chains of HPC into the pores of the oxide phase.

Reduction in the porosity of composites, as a result of polymer addition to the matrix, is also important factor in determining the mechanical property of the obtained materials. SiO_2–CaO–P_2O_5–20%HPC showed higher mechanical strength (17 MPa) when compared to SiO_2–CaO–P_2O_5–10%HPC (15 MPa) and SiO_2–CaO–P_2O_5 (9 MPa).

The morphologies of the xerogels with different amounts of HPC were characterised using SEM. It can be seen from Fig. 3 that all xerogels were characterised by a smooth surface. Depending on the type of xerogel (A, B, or C), differences in the morphology of the surface occur. The SEM images of grains xerogel A reveal a mosaic morphology of the sample areas. The surface of the matrix B has a layered morphology. The surface of the xerogel C is characterised by "fibrous" morphology. As in the case of the initial matrix A and B, the smooth surface C is dotted with small fragments of the parent material.

The X-ray diffraction profiles of the obtained xerogels are shown in Fig. 4. The samples exhibited no diffraction peaks and high background ("halos") intensity in the range of 20–30° 2θ, indicating that they are highly disordered, amorphous materials.

Table II. Physical Characterisation of Xerogel Materials

Xerogel	A	B	C
Pore diameter (4 V/A by BET) (nm)	2.01	2.00	16.09
BET surface area ($m^2\ g^{-1}$)	444.25	178.98	0.51
Micropore area ($m^2\ g^{-1}$)	141.85	111.73	0.48
Total pore volume ($cm^3\ g^{-1}$)	0.223	0.089	0.002
Micropore volume ($cm^3\ g^{-1}$)	0.068	0.054	0.00024
Mesopore volume ($cm^3\ g^{-1}$)[a]	0.155	0.035	0.00176

[a] Calculated by the difference between the total pore volume and micropore volume

Stability Tests

The chemical stability of the xerogels was assessed by examining the change in pH and conductivity of the SBF in which the xerogel samples were incubated for a period of 3 months at 37±0.1°C. For each SBF solution, a slight variation in pH value was observed over time, this variation ranged from 0.02 to 0.025 pH units (Fig. 5a). The conductivity of each SBF solution slightly increased with increased incubation time (Fig. 5b). These changes amounted to about 4 mS, for the value of conductivity about 20 mS. This can be explained by the slow release rate of silicic acid from the matrix. The lack of significant changes in pH and conductivity indicates that the obtained xerogels were chemically stable in this model medium.

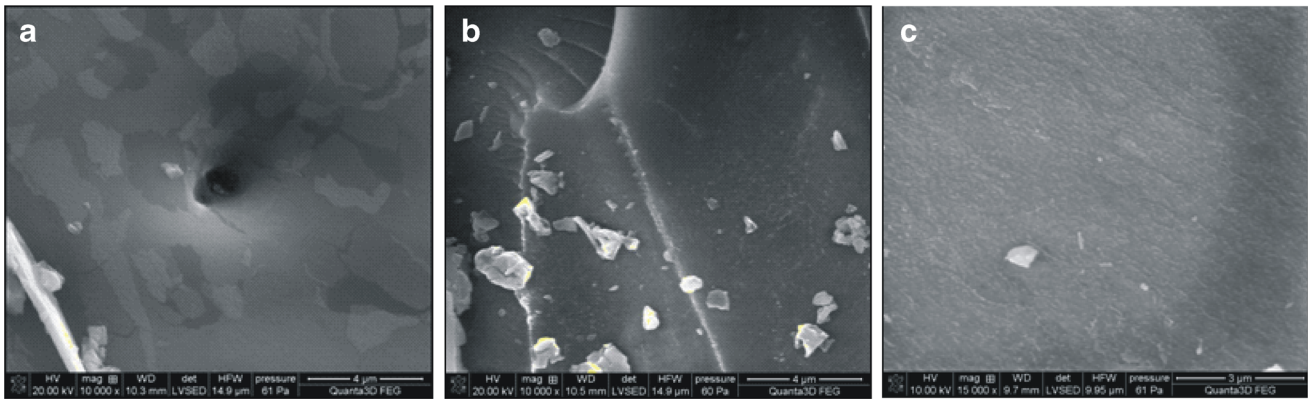

Fig. 3. SEM micrographs for SiO_2–CaO–P_2O_5 (**a**), HPC (10%)–SiO_2–CaO–P_2O_5 (**b**), and HPC (20%)–SiO_2–CaO–P_2O_5 (**c**) xerogels

In Vitro Bioactivity Test

Bioactive ceramics and glasses form a bone-like apatite layer on their surfaces after being implanted in bone. A similar bone-like apatite layer can form on bioactive materials if they are immersed in a SBF, as proposed by Kokubo and coworkers (*in vitro* Kokubo test) (18). The SBF has inorganic ion concentrations close to that of human blood plasma and does not contain any cells or proteins. In such an environment, bonelike apatite is created by the chemical reactions of the biomaterial components with the SBF ions. A high concentration of silanols (Si–OH) on the oxide surface, the presence of Ca^{2+} in the oxide network and the presence of Ca^{2+}, HPO_4^{2-} and HCO_3^- ions in the SBF solution have been shown to stimulated the formation of an amorphous calcium phosphate layer and then the carbonate–hydroxyapatite nanocrystals (HA) (24).

Samples of xerogels were incubated in SBF at 37°C for 30 days (0.5 g/50 mL). After incubation, the xerogels were dried at 80°C for 1 day and examined using FTIR, XRD and SEM-EDS techniques to determine the ability to form an apatite layer.

The FTIR spectra showed two new bands at about 550 and 600 cm^{-1} wavenumbers (the major absorption mode of the phosphate groups—the O–P–O bending mode), which indicates the formation of crystalline apatite (Fig. 6). Before incubation in the SBF, the FTIR spectra of tested xerogels showed a single, weak band observed at about 580 cm^{-1} (vibration of Si–O and P–O). However, following longer incubation of the xerogels in the SBF solution, a sharp doublet appeared at 564 and 602 cm^{-1}, indicating the formation of crystalline hydroxyapatite. Additionally, carbonate groups substituting the PO_4^{3-} ions in the apatite structure, can be detected in all xerogels by the appearance of bands at 1410–1460 cm^{-1} (25,26).

The induction period for the crystallinity of HA depends on the composition of xerogels. It was observed that the increase in the percentage of HPC in xerogels results in faster growth of hydroxyapatite on the surface of the composites. This indicates improvement of bioactive properties of composite materials. The differences in the HA growth on the xerogel surface are related to its formation mechanism. The OH– groups from oxide xerogels form hydrogen bonds with the components of the SBF solution, especially with Ca^{2+}, CO_3^{2-} and HPO_4^{2-} ions, resulting in the growth of HA on the surface of the xerogels. In the case of HPC, −OH groups in the structure of hydroxypropylcellulose probably serves as an additional nucleus of hydroxyapatite crystallisation. Hydroxypropyl cellulose as a bioadhesive polymer may further facilitate the adhesion of the inorganic ions (such as Ca^{2+}, PO_4^{3-} and CO_3^{2-}) to the surface of the xerogel matrix by hydrogen bonds formed with the components of the SBF fluid.

To confirm the ability to grow apatite on the surface of materials, XRD and SEM with EDS and mapping surface tests were performed.

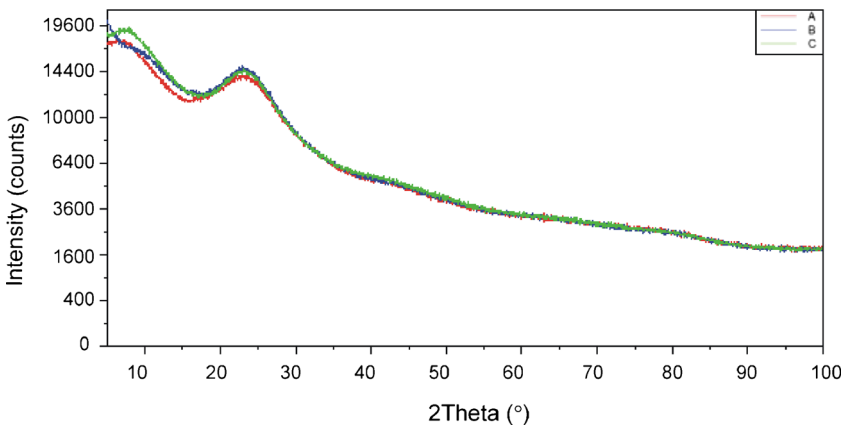

Fig. 4. The XRD patterns of the synthesised xerogels: SiO_2–CaO–P_2O_5 (**a**), HPC (10%)–SiO_2–CaO–P_2O_5 (**b**), and HPC (20%)–SiO_2–CaO–P_2O_5 (**c**)

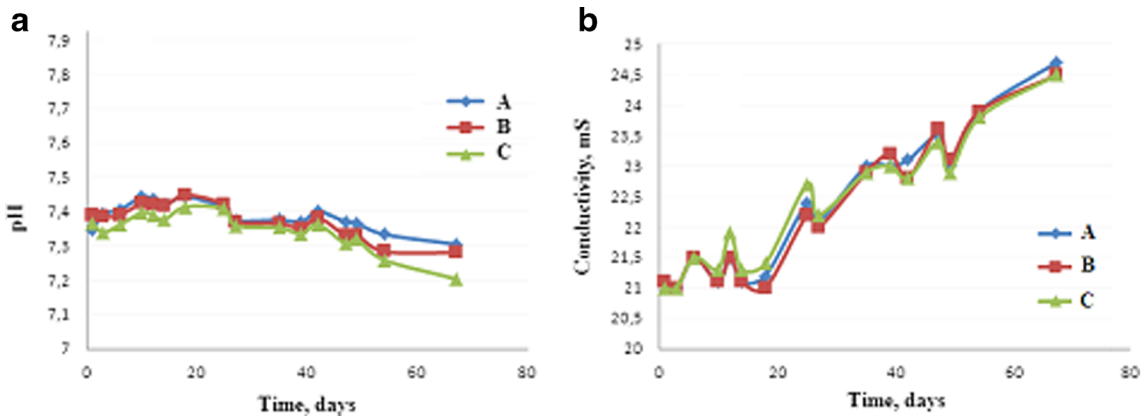

Fig. 5. The chemical stability of the xerogels: **a** pH and **b** conductivity of the SBF in which the xerogel samples were incubated for a period of 3 months

The XRD patterns for all xerogels are shown in Fig. 7. After immersion in the SBF, the X-ray diffraction analysis showed that all xerogels produced new peaks demonstrating the surface crystallisation. The most intense peaks occur at 2θ 32°, 26° which are 2 1 1 and 0 0 2 diffractions, respectively, of the apatite (according to the standard JCPDS cards 09–0432) (27). As apparent from the diffraction pattern, the content of crystalline phase decreases with increasing concentration of HPC in the oxide matrix. A lower crystallinity of apatite on the surface of the sample B and especially C indicates the formation of apatite containing carbonate substitution (confirmed by FTIR); such apatite is very poorly crystalline (natural apatite) (28).

Figure 8 shows the SEM images and EDS analysis of obtained xerogels after being soaked in SBF for 1 month. It was observed that some clustered particles or thin layer deposited on the surface of all materials. EDS analysis suggested that the Ca/P ratio of the accumulated forms on xerogels surface was 1.55–1.69, which was close to that of the hydroxyapatite (1.67).

Depending on the type of matrix, different forms of HA were created. For SiO_2–CaO–P_2O_5 xerogel, scattered aggregates of HA were formed on the surface (bright objects on maps the distribution of atoms—Fig. 8a). In the case of HPC-modified xerogels, the formation of a thin, a continuous layer rich in calcium and phosphorous on the rough surfaces composed of silica and cellulose was observed (Fig. 8b, c). The greater percentage of HPC in the oxide matrix results in a more extensive area of accumulation of hydroxyapatite. The obtained results clearly indicate that the adhesive polymer—HPC—has a beneficial impact on the bioactive properties of the final material.

Drug Release Analysis

All obtained xerogel carriers with metronidazole have sustained release profiles characterised by a faster initial release followed by a constant slow release for a period of 3–5 h (Fig. 9). A much more rapid release was demonstrated in MT–SiO_2–CaO–P_2O_5 system. Differently, the releasing of MT from HPC-modified oxide xerogels occurred in a more monotonous manner, without the pronounced initial burst of MT. The early rapid release of the drug may be related to the dissolution and diffusion process from the outermost surface of the matrix. It may be speculated that not all of the drug has been truly embedded in the xerogels, and some of it has been "squeezed-out" during the syneresis process (occurring simultaneously with the gel drying cycle), thus remaining on the

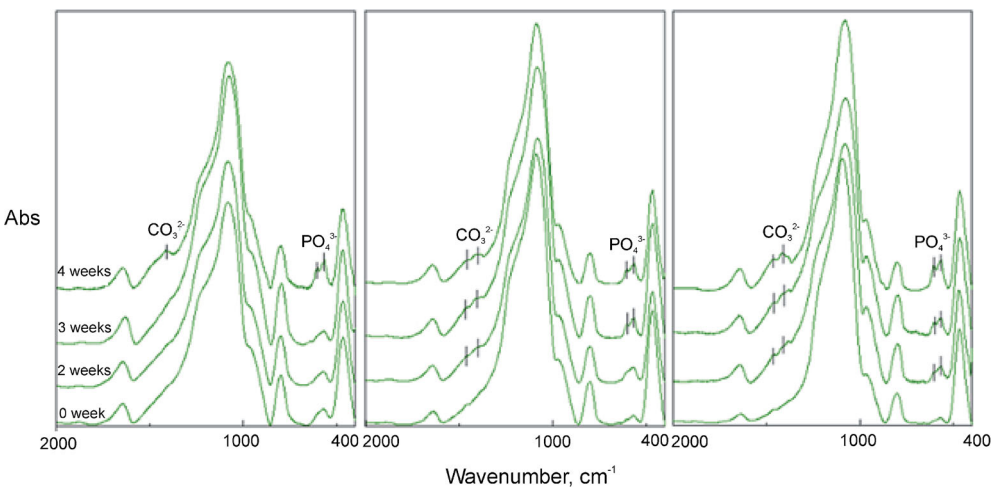

Fig. 6. FTIR spectra of **a–c** xerogel samples before and after each week of soaking in SBF solution

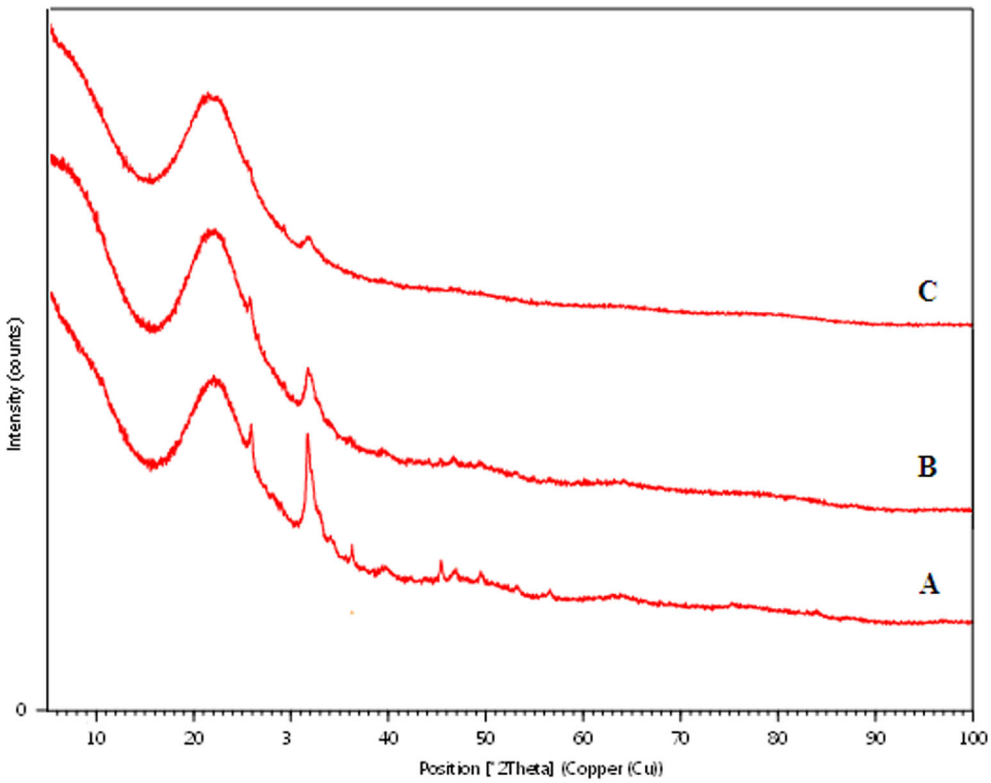

Fig. 7. The XRD patterns of the **a–c** xerogels after 1 month of soaking in SBF solution

outer surface of the matrix or close to the surface of the matrix. This fraction of the drug can be easily released into the dissolution medium in contrast to the slow release of the drug from the inner part of the matrix.

This study shows that the relative proportion of SiO_2–CaO–P_2O_5 and HPC determines the release rate of the drug. This study showed that 50% of the drug was released within the first 18 min from pure oxide, 25 and 52 min from xerogels containing 10 and 20% HPC, respectively. Complete release of the drug (96–98%) occurred within 2.75 h from pure oxide while from the HPC-modified matrices (10 and 20% HPC) within 3.25 and 4.75 h, respectively.

One of the reasons affecting the drug release rate may be the difference in porosity of the oxide and HPC-modified oxide matrices, which was observed during the BET analysis. The polymer structure of HPC has the impact on reducing the porosity of the oxide material, whereby the drug is more effectively immobilised in its pores. Additionally, hydroxypropyl cellulose swells in contact with the SBF solution and formed a viscous gel, which slows the diffusion of the drug substance from the xerogel matrix.

Another reason that may cause this phenomenon is the interactions between the drug substance and the matrix. The most important role in MT release is the hydrogen bonding between MT and the xerogel matrices. The oxide xerogels have hydroxyl groups on the surface of the pores through which they can interact (through hydrogen bonds) with the drug and thus slow down its release. The addition of HPC to the reaction mixture may increase the hydrophilicity of the surface by additional hydroxyl groups, which can interact electrostatically with the drug. In summary, HPC-oxide matrix may have reduced the release of the drug in a physical and chemical manner: through its smaller pores and swelling properties, and additionally, on account of stronger interactions with drug.

The Korsmeyer–Peppas model, an empirical exponential expression was used to determine the kinetics of the drug release rate (Eq. 1)

$$\frac{M_t}{M_\infty} = Kt^n \tag{1}$$

where M_t/M_∞ is a fraction of drug released at time t, K is the constant and n is the diffusional exponent, which characterises the release mechanism (29–31). Generally, 60% of the total amount of the drug release is fitted in this kinetic model.

Higher value of K implies a faster release. The n value closer to 1 corresponds to zero-order release kinetics, $0.5 \le n < 1$ to non-Fickian release and $n < 0.5$ to classical Fickian diffusion-controlled drug release (Higuchi model). From the plot of log $(M_t/M_\infty) = f$ (log t), kinetic parameter n was calculated, and then, from Eq. 1, constant K was determined.

The kinetics parameters of MT release rate from xerogel carriers are summarised in Table III.

The K values show that the organic modification of oxide matrix visibly affects the system release. The highest value of K for pure oxide xerogel shows the fastest release of MT from this matrix; lower values of K for xerogels with the addition of HPC show clear evidence of slower release of MT. The diffusional exponent $n < 0.5$ for all matrices indicates that MT was released from all xerogel carriers by Fickian diffusion.

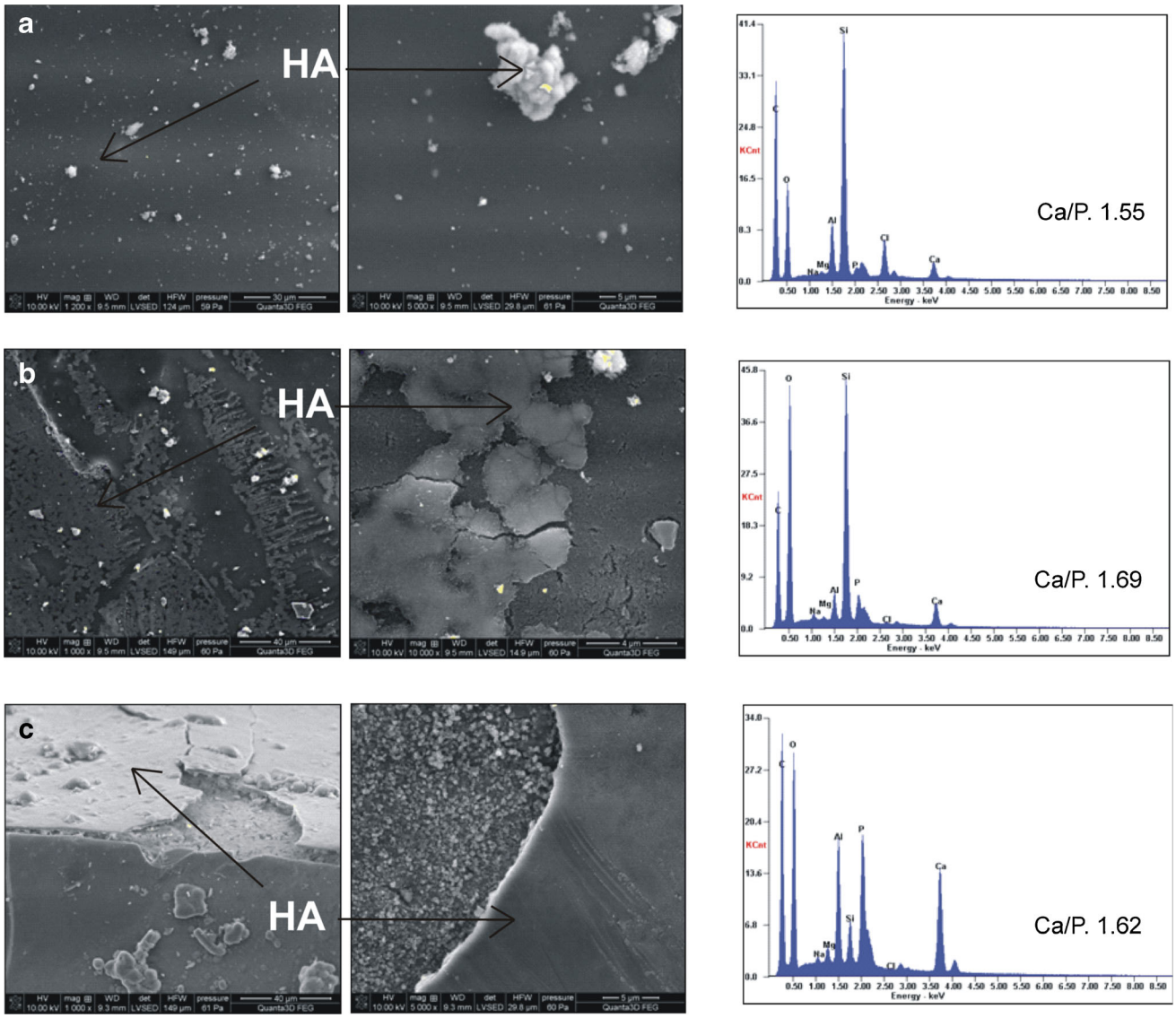

Fig. 8. The SEM images and EDS analysis of **a**–**c** xerogels after soaked in SBF for 1 month

CONCLUSIONS

In summary, it has been confirmed that it is possible to produce oxide and hybrid, polymer/oxide carrier materials for metronidazole as a model drug. Such obtained xerogels could be attractive candidates for local therapeutic applications (as drug carriers) in bone disease. The local drug release systems into the implant site have many advantages, such as high delivery efficiency, lower toxicity, continuous action and convenience for the patients.

In this study, the sol–gel prepared SiO_2–CaO–P_2O_5 and HPC–SiO_2–CaO–P_2O_5 xerogels were used as carrier matrices. The conducted experiments showed that obtained xerogels are bioactive *in vitro* and chemically stable in a simulated blood plasma solution. The addition of HPC to the oxide matrix clearly improved the bioactivity of material, due to

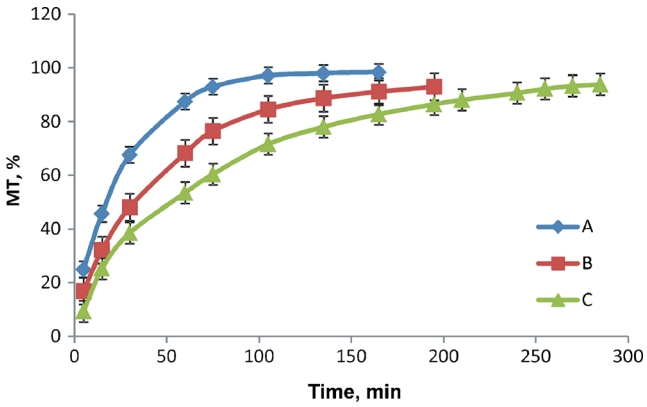

Fig. 9. The release profiles of MT from **a**–**c** xerogels, respectively

Table III. Kinetics Parameters of MT Release From Xerogel Carriers

Xerogel	n	K (% h^{-n})	R^2	Kinetics mechanism
A	0.46	70.9	0.98	Fickian diffusion
B	0.49	66.3	0.99	Fickian diffusion
C	0.38	56.0	0.99	Fickian diffusion

the ability to create electrostatic interactions with the components of the SBF solution.

The drug release data confirmed that sol–gel processed composites are efficient drug carriers for controlled release of metronidazole. A sustained release profile of the drug was achieved for all xerogel/metronidazole materials. The rate of the release of MT from xerogels was strongly correlated with the composition of the matrix. In comparison with pure oxide matrix, the HPC-modified matrices slowed down the release of MT, primarily due to decrease in xerogel porosity and, additionally, on account of stronger interactions with drug. The kinetic analysis of drug release data indicates the diffusion-controlled mechanism.

ACKNOWLEDGMENTS

This project was supported by the Ministry of Science and Higher Education of the Republic of Poland, from the quality-promoting subsidy, under the Leading National Research Centre (KNOW) programme for the years 2012–2017.

REFERENCES

1. Ahola M, Kortesuo P, Kangasniemi I, Kiesvaara J, Yli-Urpo AU. Silica xerogel carrier material for controlled release of toremifene citrate. Int J Pharm. 2000;195(1–2):219–27.
2. Czarnobaj K, Czarnobaj J. Sol–gel processed porous silica carriers for the controlled release of diclofenac diethylamine. J Biomed Mater Res Part B Appl Biomater. 2008;87(1):114–20.
3. Sieminska L, Zerda TW. Diffusion of steroids from sol–gel glass. J Phys Chem. 1996;100(11):4591–7.
4. de Gaetano F, Ambrosio L, Raucci MG, Marotta A, Catauro M. Sol–gel processing of drug delivery materials and release kinetics. J Mater Sci Mater In Med. 2005;16(3):261–8.
5. Radin S, Falaize S, Lee MH, Ducheyne P. *In vitro* bioactivity and degradation behavior of silica xerogels intended as controlled release materials. Biomaterials. 2002;23(15):3113–20.
6. Domingues Z, Cortes M, Gomes T, Diniz H, Gomes J, Faria A, *et al*. Bioactive glass as a drug delivery system of tetracycline and tetracycline associated with β-cyclodextrin. Biomaterials. 2004;25(2):327–34.
7. Tsuru K, Hayakawa S, Osaka A. Synthesis of bioactive and porous organic–inorganic hybrids for biomedical applications. J Sol–Gel Sci Tech. 2004;32(1):201–9.
8. Schmidt H. Synthesis of bioactive and porous organic–inorganic hybrids for biomedical applications. J Non-Cyst Solids. 1988;100(1–3):5156–64.
9. Buckley AM, Greenblatt M. The sol–gel preparation of silica gels. J Chem Educ. 1994;71(7):599–602.
10. Livage J, Sanchez C. Sol–gel chemistry. J Non-Cyst Solids. 1992;145:11–20.
11. Czarnobaj K, Sawicki W. The sol–gel prepared SiO_2–CaO–P_2O_5 composites doped with Metronidazole for application in local delivery systems. Pharm Dev Technol. 2012;17(6):697–704.
12. Czarnobaj K, Sawicki W. Influence of surfactants on the release behaviour and structural properties of sol–gel derived silica xerogels embedded with metronidazole. Pharm Dev Technol. 2013;18(2):377–83.
13. Zhang Y, Kim JM, Wu D, Sun Y, Zhao D, Peng S. Sol–gel synthesis of methyl-modified mesoporous materials with dual porosity. J Non-Cyst Solids. 2005;351(8–9):777–84.
14. Kortesuo P, Ahola M, Kangas M, Leino T, Laakso S, Vuorilehto L, *et al*. Alkyl-substituted silica gel as a carrier in the controlled release of dexmedetomidine. J Control Rel. 2001;76(3):227–38.
15. Granja PL, Barbosa MA, Pouyegu L, de Jeso B, Rouais F, Baquey C. Cellulose phosphates as biomaterials. Mineralization of chemically modified regenerated cellulose hydrogels. J Mater Sci. 2001;36(9):2163–72.
16. Jones D, Woolfson A, Brown A, O'Neill M. Mucoadhesive, syringeable drug delivery systems for controlled application of metronidazole to the periodontal pocket: *in vitro* release kinetics, syringeability, mechanical and mucoadhesive properties. J Control Rel. 1997;49(1):71–9.
17. Kokubo T, Kushitani H, Sakka S, Kitsugi T, Yamamuro T. Solutions able to reproduce *in vivo* surface-structure changes in bioactive glass-ceramic A-W. J Biomed Mater Res Part A. 1990;24(6):721–6.
18. Kokubo T, Takadama H. How useful is SBF in predicting *in vivo* bone activity? Biomaterials. 2006;27(16):2907–12.
19. Gross A, Chai CS, Kannangara GS, Ben-Nissan B, Hanley L. Thin hydroxyapatite coatings via sol–gel synthesis. J Mater Sci Mater Med. 1998;9(12):839–43.
20. Rezwan K, Chen QZ, Blaker JJ, Boccaccini AR. Biodegradable and bioactive porous polymer/inorganic composite scaffolds for bone tissue engineering. Biomaterials. 2006;27(17):3413–8.
21. Al-Oweini R, El-Rassy H. Synthesis and characterization by FTIR spectroscopy of silica aerogels prepared using several Si $(OR)_4$ and RSi $(OR)_3$ precursors. J Mol Struct. 2009;919(1–3):140–5.
22. Fidalgo A, Ilharco L. Correlation between physical properties and structure of silica xerogels. J Non-Cyst Solids. 2004;347(1–3):128–33.
23. Bryans T, Brawner V, Quitevis E. Microstructure and porosity of silica xerogel monoliths prepared by the fast sol–gel method. J Sol–Gel Sci Tech. 2000;17(3):211–6.
24. Palazzo B, Iafisco M, Laforgia M, Margiotta N, Natile G, Bianchi CL, *et al*. Biomimetic hydroxyapatite-drug nanocrystals as potential bane substitutes with antitumor drug delivery properties. Adv Funct Mater. 2007;17(13):2180–8.
25. Łączka M, Cholewa-Kowalska K, Kulgawczyk K, Klisch M, Mozgawa W. Structural examinations of gel-derived materials of the CaO–P_2O_5–SiO_2 system. J Mol Struct. 1999;511–512:223–30.
26. Łączka M, Cholewa K, Łączka-Osyczka A. Organic–inorganic hybrid glasses of selective optical transmission. J Alloys Compd. 1997;248(1–2):42–7.
27. Li N, Jie Q, Zhu S, Wang R. Preparation and characterization of macroporous sol–gel bioglass. Ceram Int. 2005;31(5):641–6.
28. Ibrahim DM, Mostafa AA, Korowash SI. Chemical characterization of some substituted hydroxyapatites. Chem Cent J. 2011;5(1):74–85.
29. Böttcher H, Slowik P, Böttcher H, Slowik P, Süβ W. Sol–gel carrier systems for controlled drug delivery. J Sol–Gel Sci Tech. 1998;13(1):277–82.
30. Costa P, Sousa Lobo JM. Modeling and comparison of dissolution profiles. Eur J Pharm Sci. 2001;13(2):123–7.
31. Peppas N. Analysis of Fickian and non-Fickian drug release from polymers. Pharm Acta Helv. 1985;60(4):110–5.